

Supplement of *Clim. Past*, 17, 1005–1023, 2021
<https://doi.org/10.5194/cp-17-1005-2021-supplement>
© Author(s) 2021. CC BY 4.0 License.



Supplement of

Large-scale climate signals of a European oxygen isotope network from tree rings

Daniel F. Balting et al.

Correspondence to: Daniel F. Balting (daniel.balting@awi.de)

The copyright of individual parts of the supplement might differ from the article licence.

<i>Location</i>	<i>Country</i>	<i>Species</i>	<i>Altitude</i>	<i>Lat.</i>	<i>Lon.</i>	<i>First year</i>	<i>Last year</i>
<i>Carzola</i>	Spain	<i>Pinus nigra</i>	1820 m	37.53°	-2.57°	1600	2002
<i>Caveragno</i>	Switzerland	<i>Quercus petraea</i>	900 m	46.21°	8.36°	1637	2002
<i>Col Du Zad</i>	Morocco	<i>Cedrus atlantica</i>	2200 m	32.59°	-5.14°	1600	2000
<i>Dransfeld</i>	Germany	<i>Quercus petraea</i>	320 m	51.50°	9.78°	1776	2002
<i>Fontainebleau</i>	France	<i>Quercus petraea</i>	100 m	48.38°	2.67°	1600	2000
<i>Gutuli</i>	Norway	<i>Pinus sylvestris</i>	800 m	62.00°	12.18°	1600	2003
<i>Inari</i>	Finland	<i>Pinus sylvestris</i>	150 m	68.93°	28.42°	1600	2002
<i>Isibeli</i>	Turkey	<i>Juniper excelsa</i>	1800 m	37.06°	30.45°	1850	2005
<i>Laizer</i>	Austria	<i>Quercus petraea</i>	300 m	48.18°	16.20°	1600	2003
<i>Lochwood</i>	United Kingdom	<i>Quercus petraea</i>	175 m	55.27°	-3.43°	1749	2003
<i>Monte Pollino</i>	Italy	<i>Pinus leucodermis</i>	1900 m	39.58°	16.16°	1604	2003
<i>Mount Vichren</i>	Bulgaria	<i>Pinus heldreichii</i>	1900 m	41.46°	23.24°	1800	2005
<i>Naklo</i>	Slovenia	<i>Larix decidua</i>	440 m	46.30°	14.30°	1600	2005
<i>Niepolomice</i>	Poland	<i>Quercus robur</i> & <i>Pinus sylvestris</i>	190 m	50.12°	20.38°	1627	2003
<i>Panemunės</i>	Lithuania	<i>Pinus sylvestris</i>	45 m	54.88°	23.97°	1816	2002
<i>Pedraforca</i>	Spain	<i>Pinus uncinata</i>	2120 m	42.13°	1.42°	1600	2003
<i>Pinar de Lillo</i>	Spain	<i>Pinus sylvestris</i>	1600 m	42.57°	-5.34°	1600	2002
<i>Plieningen</i>	Germany	<i>Quercus petraea</i>	340 m	48.42°	9.13°	1822	1999
<i>Poellau</i>	Austria	<i>Pinus nigra</i>	500 m	47.95°	16.06°	1600	2002
<i>Rennes</i>	France	<i>Quercus robur</i>	100 m	48.25°	-1.7°	1751	1998
<i>Sivakkovaara</i>	Finland	<i>Pinus sylvestris</i>	200 m	62.98°	30.98°	1600	2002
<i>Suwalki</i>	Poland	<i>Pinus sylvestris</i>	160 m	54.10°	22.93°	1600	2004
<i>Vigera</i>	Switzerland	<i>Pinus sylvestris</i>	1400 m	46.50°	8.77°	1675	2003
<i>Vinuesa</i>	Spain	<i>Pinus uncinata</i>	720 m	42.00°	2.45°	1850	2002
<i>Woburn</i>	United Kingdom	<i>Pinus sylvestris</i>	10 m	51.98°	-0.59°	1604	2003

Table S1: The characteristics of each sample site which is used within our study. 22 of the 26 $\delta^{18}\text{O}_{\text{cel}}$ records were created within the EU project ISONET (Treydte et al., 2007a, b) and four additional sites from Bulgaria, Turkey, Southwest Germany and Slovenia were added (Hafner et al., 2014; Heinrich et al., 2013).

EOF2 JJA - OWDA
Explained Variance - 16.1%

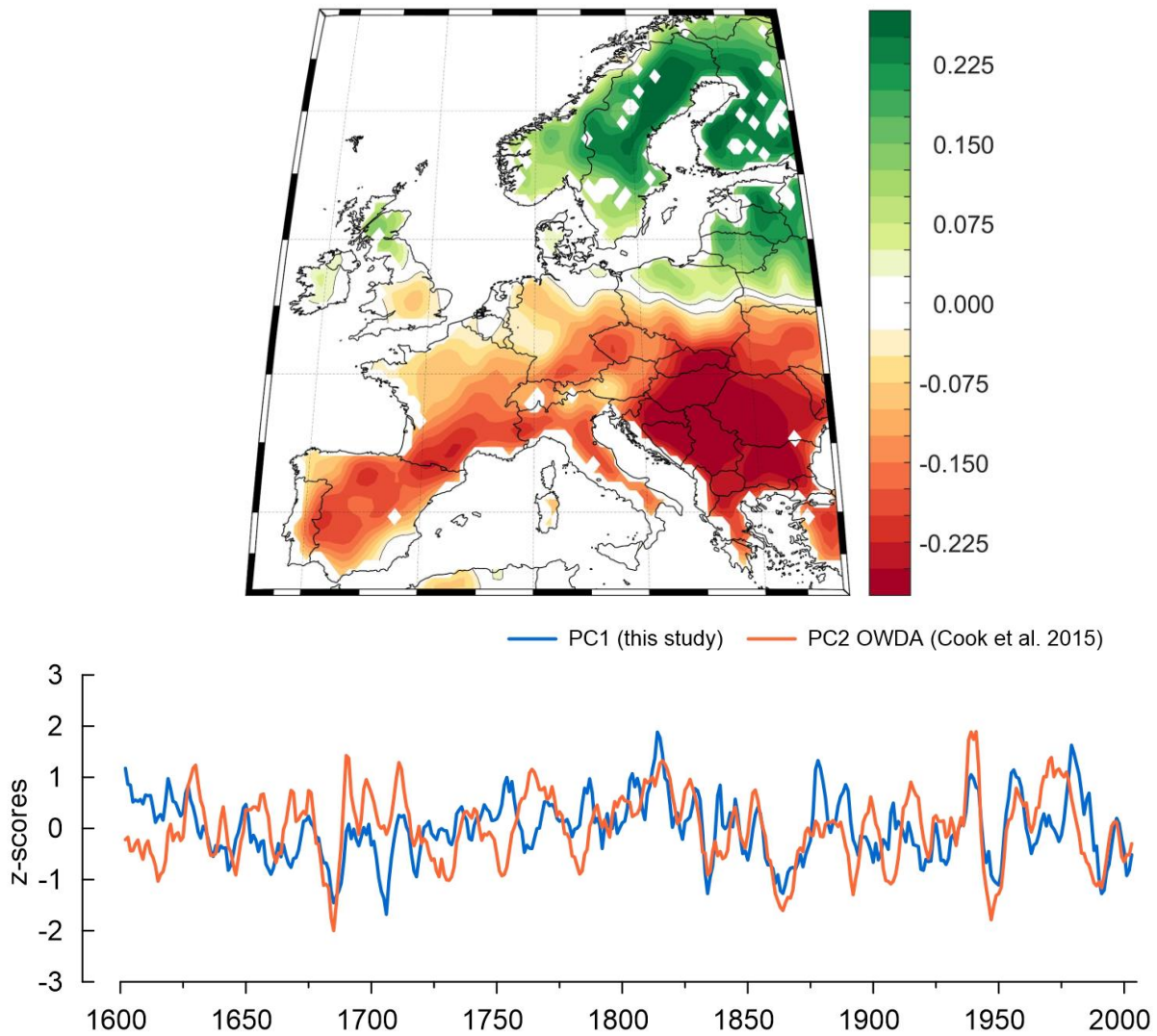


Figure S1: Upper panel: The second EOF of the OWDA (Cook et al., 2015) for JJA (explaining 16.1% of the variance). Lower panel: The associated PC2 of the OWDA for JJA and PC1 of our study. The correlation between the two time series is $R=0.39$ ($p\text{-value}=4.2e^{-16}$).

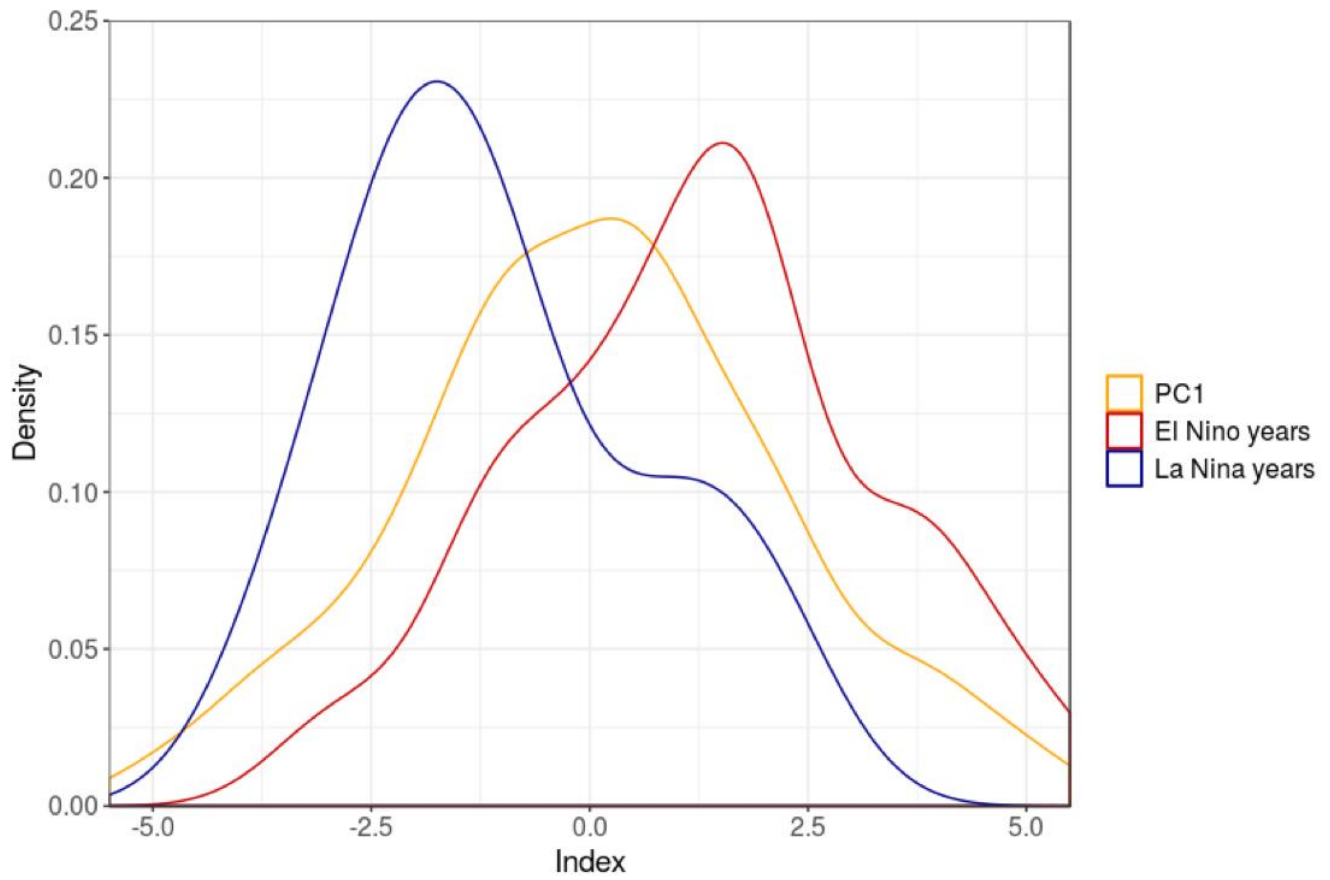


Figure S2: The probability density function of PC1 with two additional functions for El Niño and La Niña years. The El Niño and La Niña years have been extracted out of a Niño 3.4 DJF index (HadISST1; Rayner et al. 2003) for the period from 1870 to 2000.

30

35

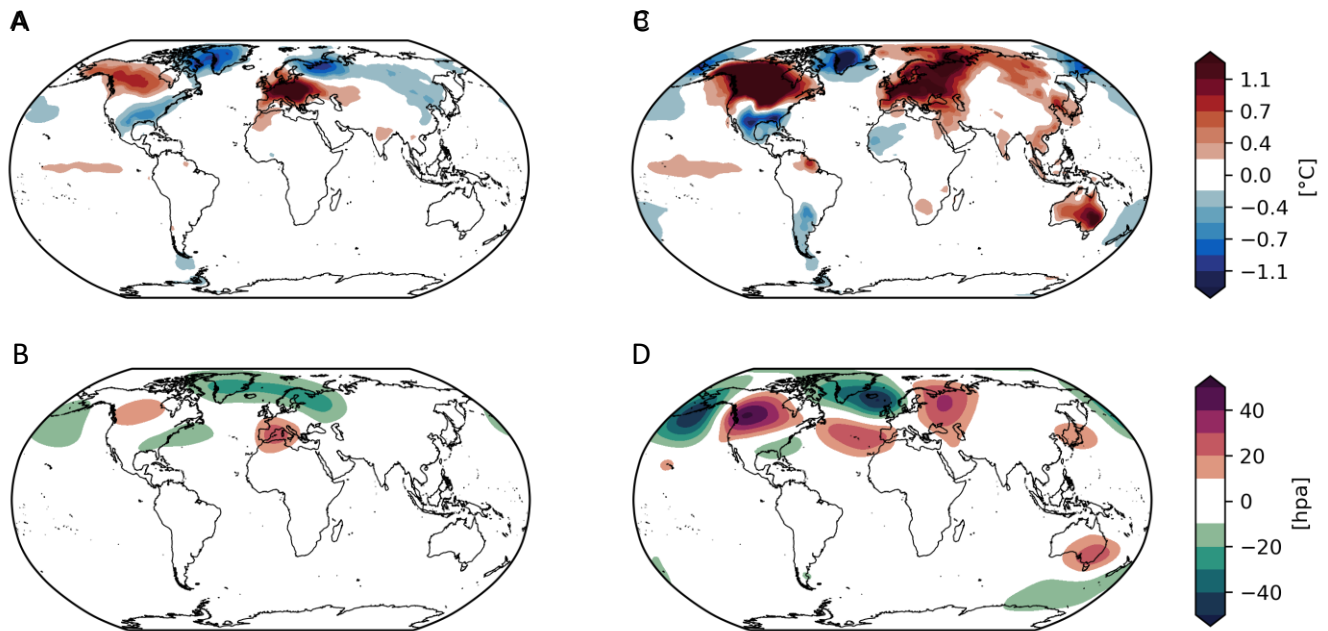
40

45

	LI ET AL. 2011	LI ET AL. 2013	DÄTWYLER ET AL. 2019
1750-1849	r=0.121 p-value=0.231	r=-0.008 p-value=0.936	r=-0.078 p-value=0.442
1850-1949	r=0.223 p-value=0.026	r=0.303 p-value=0.002	r=0.296 p-value=0.003

Table S2: Correlation between the first component of the $\delta^{18}\text{O}_{\text{cel}}$ network with three different ENSO reconstructions for two different time periods.

50



55 **Figure S3: Composite maps (high-low) for air temperature and Z500 from the Ensemble Kalman Fitting Paleo-Reanalysis**
Version 2.0 (Franke et al., 2020) for winter related to the NDJ Niño3.4 index by Li et al. (2013). The first column shows the
 characteristics of air temperature (A, C) and the second Z500 (B, D) whereas the first row shows the results for the period 1750 to 1849
 and the second for the period 1850 to 1949. The Z500 pattern over the North Atlantic shows similarities to the NAO (D) which can't be
 identified in the period before (B). The differences are also shown in the pattern of air temperature. The comparison of the two different
 periods suggests that the influence of ENSO variability on the European climate could change over time which is shown by different air
 60 temperature and Z500 patterns.

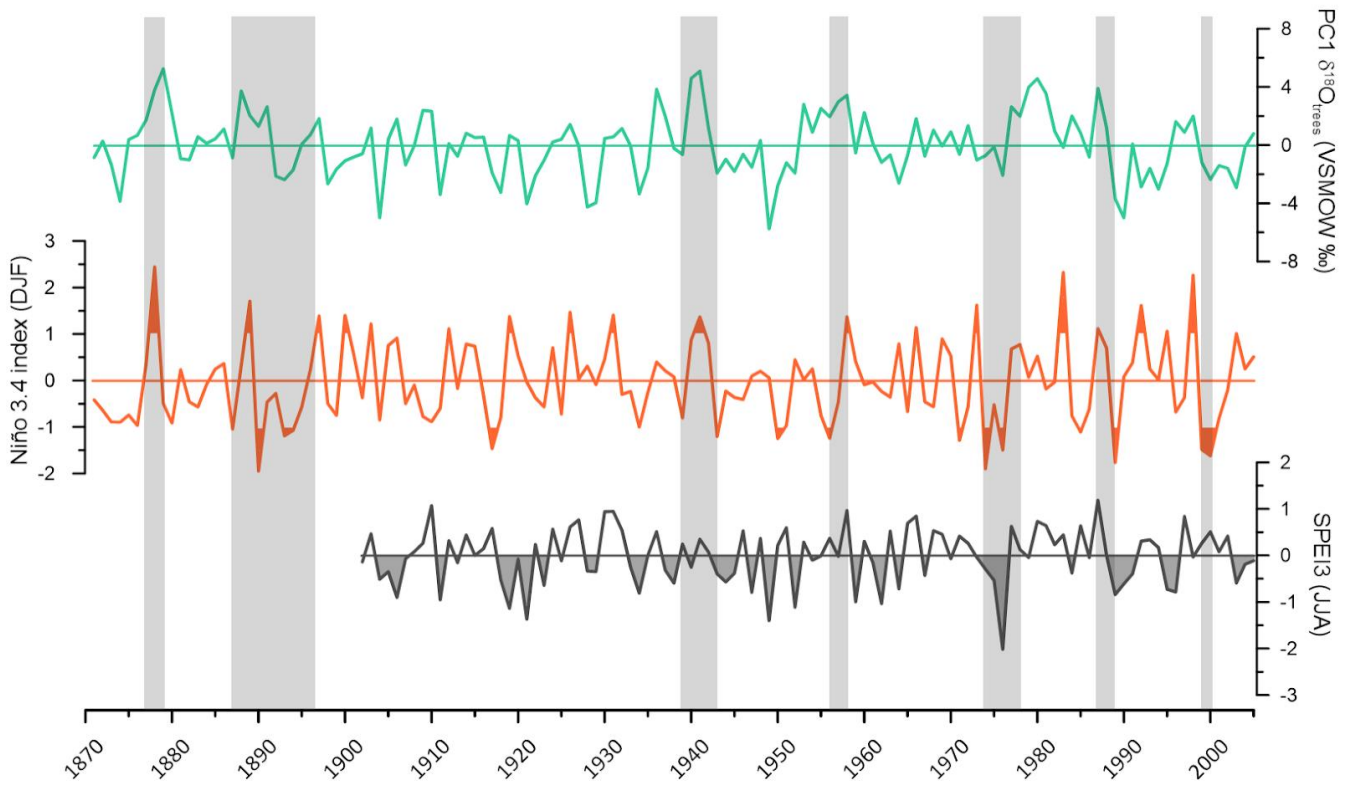
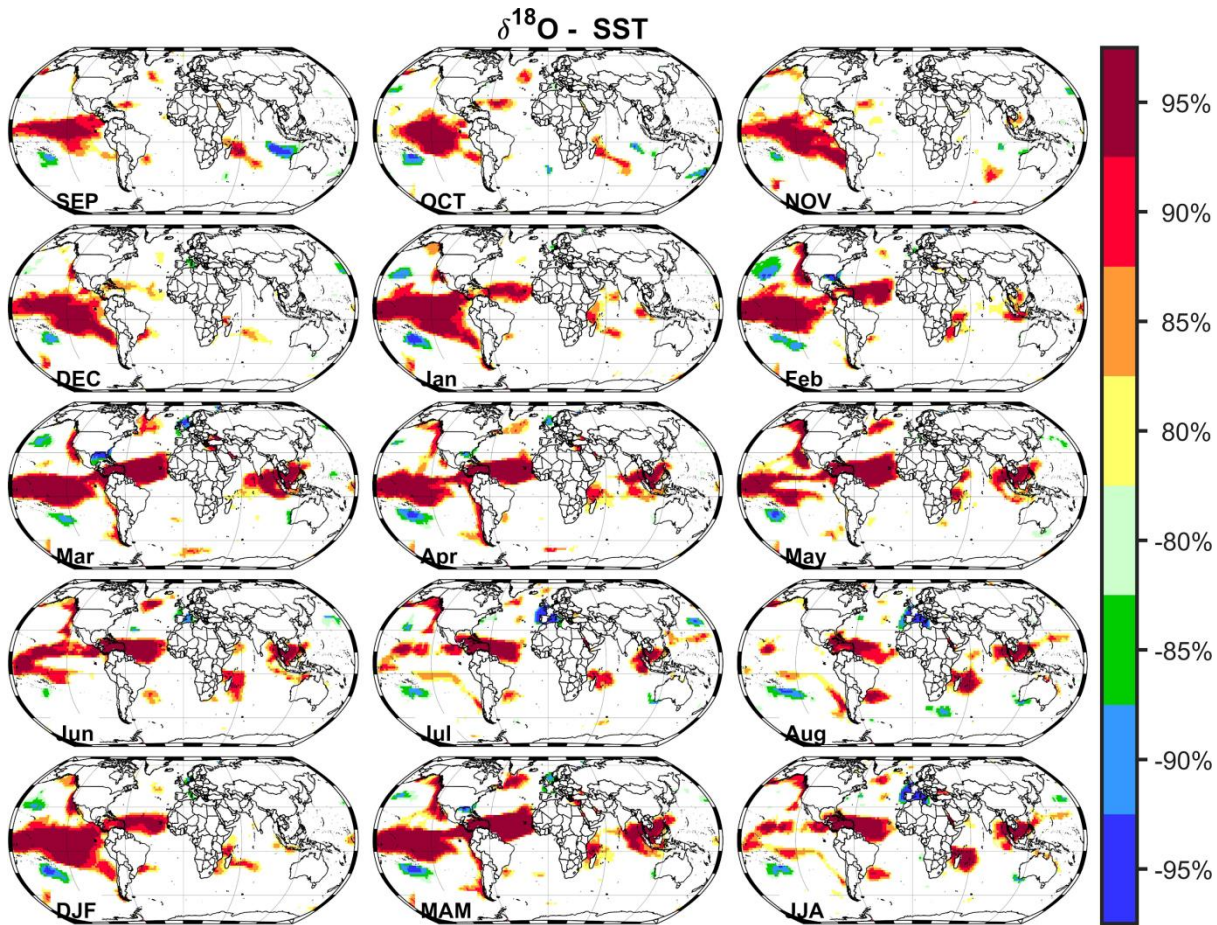


Figure S4: The time series of the first component of the stable oxygen isotope network in comparison to other time series of climate patterns. For a better comparison, a Niño 3.4 index for DJF (HadISST1; Rayner et al. 2003) and a SPEI3 drought index (SPEIbase v.2.5 [SPEI3]; Longitude -5° to 10° /Latitude 46° to 52°) are shown. Selected El Niño and La Niña events are highlighted via a grey background.

65



70 **Figure S5: Stability maps for the correlation between SST anomalies (Huang et al., 2017) and the first mode of $\delta^{18}\text{O}_{\text{cel}}$.** In order to show how stable the connection between the sea surface temperature (SST) of the tropics and the first mode of $\delta^{18}\text{O}_{\text{cel}}$ is, we have computed the stability maps of the correlation between these two quantities. The stability map is a tool which is primarily used for streamflow predictions to identify stable teleconnection (for more details see Rimbu et al. 2005 or Ionita and Nagavciuc (2020)). SST anomalies from the ERSST have been correlated with the first mode of $\delta^{18}\text{O}_{\text{cel}}$ in a moving window of 31 years. The correlation is considered to be stable for those grid points where anomalies are significantly correlated at the 90% level for more than 80% of the 31-year windows, covering the period 1854–2005. The color bar indicates how many years are characterized by a significant correlation (at the 90% level) in a 21-yr window, covering the period 1854–2005. Positive correlations are shown from yellowish to reddish and negative correlations from greenish to blueish. As it can be inferred from Supp. 6, one of the largest locations with stable correlations is located in the tropical Pacific. Stable correlations are shown from September (last year) to June which also supports our result that $\delta^{18}\text{O}_{\text{cel}}$ is able to capture a multi-seasonal signal and that the first mode of $\delta^{18}\text{O}_{\text{cel}}$ is sensitive for ENSO variability. Based on these results, we suggest that the relation between the first mode of $\delta^{18}\text{O}_{\text{cel}}$ and the SST in the tropical Pacific/Atlantic in winter and spring is stable in the period from 1854 to 2005.

75

80